Rocznik Ochrona Środowiska

Volume 26 Year 2024 ISSN 2720-7501 pp. 403-412

https://doi.org/10.54740/ros.2024.039 open access

Received: May 2024 Accepted: August 2024 Published: September 2024

Numerical Modeling of Thermal Energy Flow Compared with Data Obtained from an Experiment

Jarosław Chodór[1], Grzegorz Chomka[2], Magdalena Orłowska[3]*

[1]Branch of Koszalin University of Technology in Szczecinek, Poland

https://orcid.org/0000-0001-7153-7946

[2]Branch of Koszalin University of Technology in Szczecinek, Poland

https://orcid.org/0000-0003-1156-2108

[3]Faculty of Civil, Environmental and Geodesy Engineering, Koszalin University of Technology, Poland

https://orcid.org/0000-0002-2072-1791

corresponding author's e-mail: jaroslaw.chodor@tu.koszalin.pl

Abstract: The article presents the results of numerical analyses of temperature distribution and heat flow distribution in the building partition. The analysis results were compared with the results of the real object. A very good convergence of the results was observed.

Keywords: numerical modelling, heat transfer, thermal conductivity coefficient, temperature distribution, distribution of heat flux

1. Introduction

The currently applicable regulations regarding the required Technical Conditions from 2021 and the Journal of Laws of the Republic of Poland (2022) carry several requirements. The article refers to the external walls of the building. Materials used to build walls must meet high requirements regarding the heat transfer coefficient U W/m^{2}K. From 2021, it must not exceed 0.2 W/m^{2}K.

Individual layers in the wall should ensure the lowest possible heat loss and be characterised by appropriate thermal conductivity coefficients λ W/mK. The thickness of individual layers in a multilayer partition, the places where materials are joined, and the methods of bricklaying are also important. Welds and mortars have worse thermal insulation parameters than individual materials in wall layers.

Thermal resistance - the inverse of the thermal conductivity (1):

$$R = \frac{d}{\lambda}, \tag{1}$$

where:
R – thermal resistance, m^{2}K/W,
d – material layer thickness, m,
λ – thermal conductivity coefficient, W/mK.

Heat transfer coefficient U W/m^{2}K has a form (2)

$$U = \frac{1}{R_{si}+\sum R+R_{se}}, \tag{2}$$

where:
R_{si} – thermal resistance on the inside of the partition, m^{2}K/W,
$\sum R$ – the sum of thermal resistance from individual layers building the wall, m^{2}K/W,
R_{se} – thermal resistance on the external of the partition, m^{2}K/W.

According to PN-EN ISO 6946:2008 and Guzik (2015) directions of heat fluxes take the following values in Table 1.

Table 1. Directions of heat flow

Thermal resistance R [m^{2}K/W]	Directions of heat flow		
	Vertical up	Horizontal	Vertical down
R_{si} [m^{2}K/W]	0.1	0.13	0.17
R_{se} [m^{2}K/W]	0.4		

The given values R_{si} and R_{se} apply to the case of contact of the partition with air on both the external and internal sides.

Figure 1 shows a multilayer partition. The partition is surrounded by air on the left and right sides. The temperature t_{w1} is higher than t_{w4} and drops along the lines t_{w1}, t_{w2}, t_{w3} to t_{w4}. The thicknesses of individual layers are marked d_1,d_2,d_3, the heat conduction coefficients for individual material layers are marked λ_1, λ_2, λ_3. The direction of heat flow q is marked with an arrowhead.

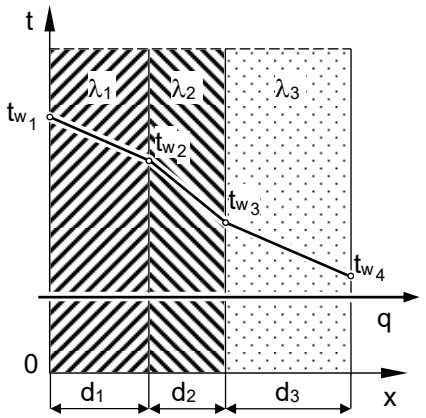

Fig. 1. Temperature distribution through a multilayer partition

The heat flux density q W/m^2 for each layer for the steady case and the homogeneous layer can be described by the following equations:

$$q = \frac{\lambda_1}{d_1} \cdot \left(t_{w1} - t_{w2}\right), \tag{3}$$

$$q = \frac{\lambda_2}{d_2} \cdot \left(t_{w2} - t_{w3}\right), \tag{4}$$

$$q = \frac{\lambda_3}{d_3} \cdot \left(t_{w3} - t_{w4}\right), \tag{5}$$

From each of these equations (3-5), the temperature difference is determined:

$$t_{w1} - t_{w2} = q \cdot \frac{d_1}{\lambda_1}, \tag{6}$$

$$t_{w2} - t_{w3} = q \cdot \frac{d_2}{\lambda_2}, \tag{7}$$

$$t_{w3} - t_{w4} = q \cdot \frac{d_3}{\lambda_3}. \tag{8}$$

After summing equations (6-8) side by side, we get:

$$t_{w1} - t_{w2} + t_{w2} - t_{w3} + t_{w3} - t_{w4} = q \cdot \left(\frac{d_1}{\lambda_1} + \frac{d_2}{\lambda_2} + \frac{d_3}{\lambda_3}\right), \tag{9}$$

where:

$$q = \frac{t_{w1} - t_{w4}}{\sum_{i=1}^{3} \frac{d_i}{\lambda_i}}. \tag{10}$$

In the case of a multilayer wall (n), the general formula for the heat flux density takes the following form (Charun 2009):

$$q = \frac{t_{w1} - t_{w,n+1}}{\sum_{i=1}^{n}\left(\frac{d}{\lambda}\right)_i} = \frac{t_{w1} - t_{w,n+1}}{\sum_{i=1}^{n} R_{\lambda_i}}. \tag{11}$$

The temperature distribution is a straight line along the wall cross-section (Figure 1).

The component $\sum_{i=1}^{n} R_{\lambda_i}$ is the sum of the heat transfer resistances from individual wall layers.

Establishing a mathematical and physical model for heat conduction in each material layer is a complex task. An important issue is determining boundary and initial conditions, whether the process is steady or unsteady, the number of dimensions, the stability or variability of thermophysical properties, the presence or absence of additional heat sources, and the conditions of heat transfer inside and on the considered surfaces. The law of heat conduction, differential energy balance equations, and uniqueness conditions influence the mathematical model. The inclusion of the above in the constraints of mathematical analysis is long-lasting. Numerical methods for unsteady heat conduction can be used to solve this type of task. For example, one of these methods is the finite difference method, where the object is divided by a mesh into a finite number of parts with a specific area or volume with dimensions appropriate to the discretisation steps. In differential equations, partial derivatives are replaced by difference quotients. The number of equations corresponds to the number of mesh nodes. Finite element methods are popular and successfully used with computers worldwide. They often enable verification of long-term experimental research or learning about complex issues (Wiśniewski & Wiśniewski 2017).

According to Fourier's law the heat flux density is directly proportional to the temperature gradient (12):

$$q = -\lambda grad T = -\lambda \nabla T, \tag{12}$$

where: ∇ – nabla operator

Heat flows as the temperature decreases, hence the minus sign.

The component of the heat flux density in the x-axis direction is given by (13):

$$q_x = -\lambda \frac{\partial T}{\partial x}. \tag{13}$$

The temperature change in the temperature field in the direction perpendicular to the thermal surface is the largest. The temperature gradient determines this change and is a vector with the form of rectangular coordinates (14):

$$\nabla T = l_x \frac{\partial T}{\partial x} + l_y \frac{\partial T}{\partial y} + l_z \frac{\partial T}{\partial z}, \tag{14}$$

where:
l – unit vectors of the coordinate system axes.

The differential equation for unsteady heat conduction in solids is the Fourier-Kirchhoff equation (15):

$$\frac{\partial T}{\partial t} = a\nabla^2 T + \frac{1}{\rho c_p}\frac{\partial \lambda}{\partial T}\left[\left(\frac{\partial T}{\partial x}\right)^2 + \left(\frac{\partial T}{\partial y}\right)^2 + \left(\frac{\partial T}{\partial y}\right)^2\right] + \frac{q_v}{\rho c_p}, \tag{15}$$

where:
a – temperature equalisation factor (16):

$$\mathrm{a} = \frac{\lambda}{\rho c_p}, \tag{16}$$

ρ – density [kg/m^3],
c_p – specific heat [J/kgK],
q_v – efficiency of the volumetric internal heat source and is given by (17):

$$q_v = \frac{d^2 Q_w}{dV dt}, \tag{17}$$

where:
Q_w – internal heat source [W],
V – volume [m^3]. (Wiśniewski & Wiśniewski 2017)

Buildings should be energy-efficient. Appropriate thermal insulation will retain heat inside the building and limit its losses to the surroundings. Thermal bridges are also places for heat to escape.

Since a large area of building partitions are external walls, these losses can reach up to about 30%. In addition to heat losses through penetration, we also have ventilation heat losses, which constitute about 35%, through the roof up to 30%, through windows about 20%, through the floor on the ground about 5% (Figure 2) (https://www.isover.pl/porady/zatrzymaj-cieplo-w-domu).

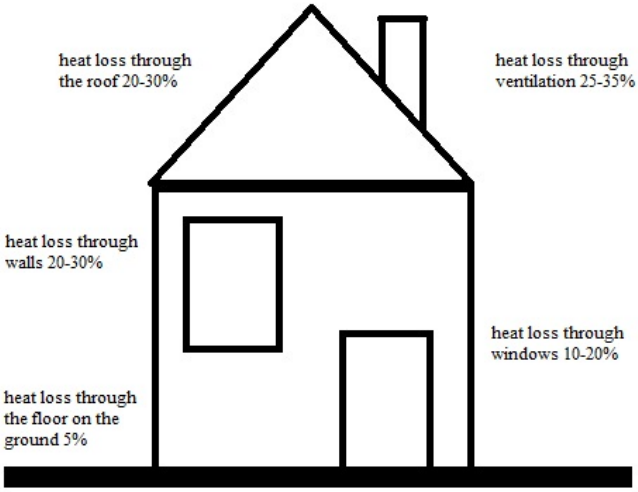

Fig. 2. Heat loss for the house

Thermal insulation materials should meet the requirements of PN-EN 13172:2012 (2012). In addition to the appropriate thermal conductivity coefficient, they should be moisture-resistant, tolerate temperature "shocks" both in summer and winter and be flexible and mechanically durable. The most common insulating filling is glass or rock mineral wool, polystyrene (including graphite and extruded polystyrene), or polyurethane boards. Materials with low thermal insulation require greater thicknesses, which results in an unfavourable appearance of the windows concerning the wall thickness, the so-called hollow effect.

The values of thermal conductivity coefficients λ for various material layers can be found in the PN-EN ISO10456:2009 (2009). The standard presents methods for determining declared and calculated thermal values for thermally homogeneous building materials and products, including procedures for converting values obtained in various conditions. The methodology covers the calculated ambient temperature range from -30°C to +60°C. Conversion factors for temperature and humidity are applied in the average temperature range from 0°C to +30°C PN-EN ISO10456:2009 (2009).

2. Numerical Analysis

Numerical analyses using the Finite Element Method (FEM) were carried out for an exterior wall constructed of materials that conform to the specifications indicated in Figure 3 and Figure 4.

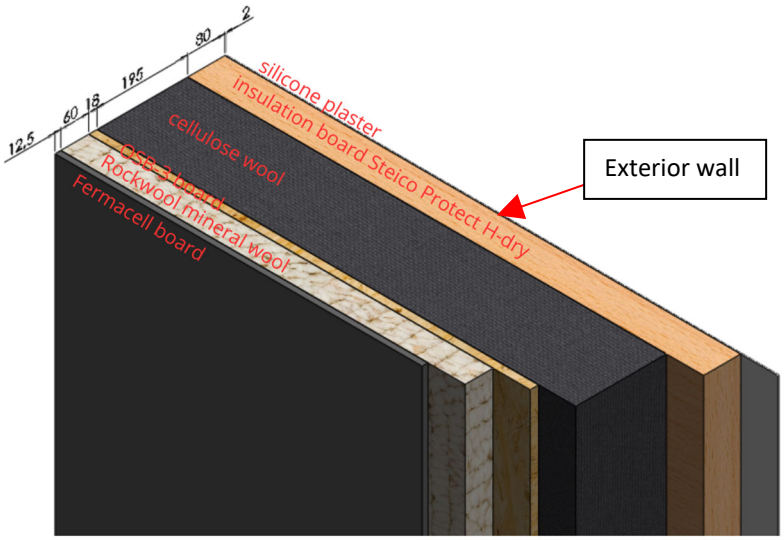

Fig. 3. Cross-section of an exterior wall with the indicated thicknesses of the individual partitions

Figure 4 shows the structure of the exterior wall, in a dilated view, with the characteristic thicknesses of its individual partitions given in the figure's description.

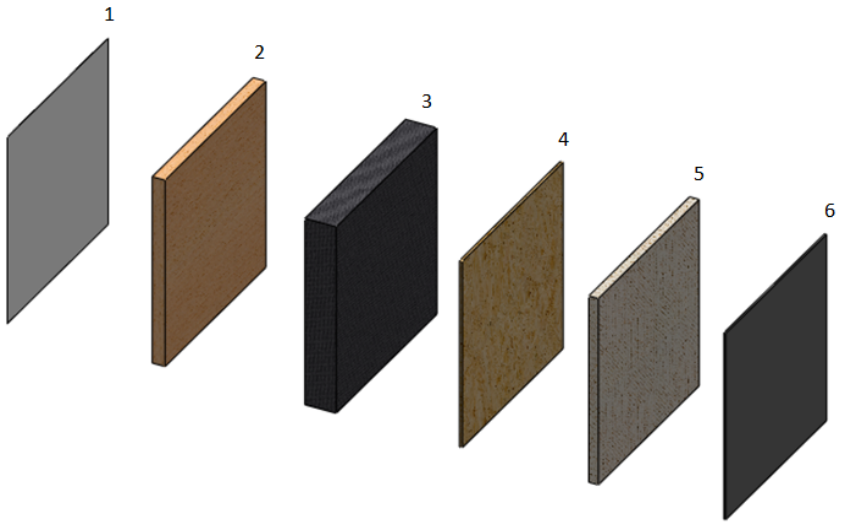

Fig. 4. Structure of the external wall model: 1) Termoorganika white silicone plaster (glue+grid+plaster) 2 mm, 2) Steico Protect H-dry 80 mm, 3) structure filled with cellulose wool 195 mm, 4) OSB-3 18 mm, 5) Rockwool 60 mm, 6) Fermacell 12.5 mm

3. Assumptions and Simplifications

The simulation aims to determine the value and direction of heat transfer in each partition layer in the configuration shown in Chapter 2 of this article.

In the simulations carried out, it was assumed, following the assumptions of ITS company, that the variant of the analysed partition consists of the following 6 layers (given from the outside):

1. silicone plaster white Termoorganika,
2. insulation board Steico Protect H-dry,
3. structure filled with cellulose wool,
4. OSB-3 board,
5. rockwool,
6. Fermacell board.

A suitable material model was selected for each layer (Table 2).

Table 2. Coefficients and material parameters used in the simulations

Lp.	Material	Thickness	Thermal conductivity coefficient	Diffusion resistance coefficient	Density of the material	Specific heat	Specific thermal resistance
		mm	W/(mK)	–	kg/m^3	J/(kgK)	m^{2}K/W
1.	Silicone plaster	2	0.7	50	1970	750	0.002
2.	Steico protect H-dry 80 mm board	80	0.048	5	265	2100	1.666
3.	cellulose wool 195 mm	195	0.038	3	33.8	2150	5.131
4.	OSB 3 th. 18 mm	18	0.13	50	650	1700	0.138
5.	Rockwool rock wool 60 mm	60	0.033	1	50	840	1.818
6.	Fermacell board 12.5 mm	12.5	0.32	16	1150	1000	0.039

It was assumed that the models are isotropic and the process of heat transfer occurs in the temperature range set at the extreme layers of the partition and are, respectively:
External side, silicone plaster (-15°C, -10°C, -5°C, 0°C, +5°C, +10°C, +15°C, +20°C, +25°C),
Fermacell board, constant temperature (+21°C).

The assumed values reflect indoor temperatures (+21°C) with assumed outdoor adverse weather conditions (temperature range from -15°C to +25°C simulating temperatures throughout the calendar year). Nine computer simulations were carried out.

4. Computer Model for All Temperature Variants Analysed

Figure 5 shows the discretised computer model of the analysed wall current for all analysed temperature variants. The dimensions of the analysed wall are 1200 mm × 1200 mm.

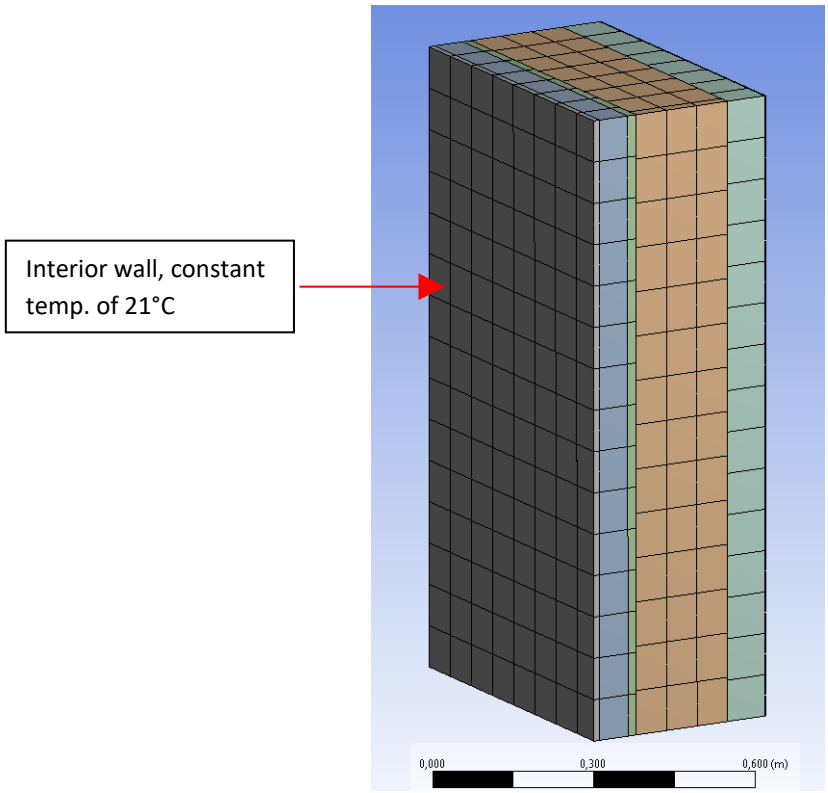

Fig. 5. Discrete model of a multilayer wall

The boundary-initial conditions for all analysed models were set at the extreme surfaces of the partition under study, intended to reflect the temperatures prevailing outside and inside the partition. The preset values in the simulations are as follows:
- Silicone plaster (-15°C, -10°C, -5°C, 0°C, +5°C, +10°C, +15°C, +20°C, +25°C),
- Fermacell board, constant temperature (+21°C).

The set time in each simulation was 172800 seconds, corresponding to 48 hours. For such a time interval, all results are presented.

Sample results are shown below in figures for the temperature variant (-15°C). Aggregate results for each temperature variant are shown in the form of graphs.

Based on the simulations and the results obtained, a decrease in temperature on the residential side was observed after 48 hours from 21°C to a value of about 11°C. Measurements in the center of the tested partition on the residential side indicated very similar temperatures over the entire surface, amounting to, respectively, 11.008°C, 11.001°C and 11°C (Figure 6) after 48 hours (slight differences in temperature indications are the result of numerical error).

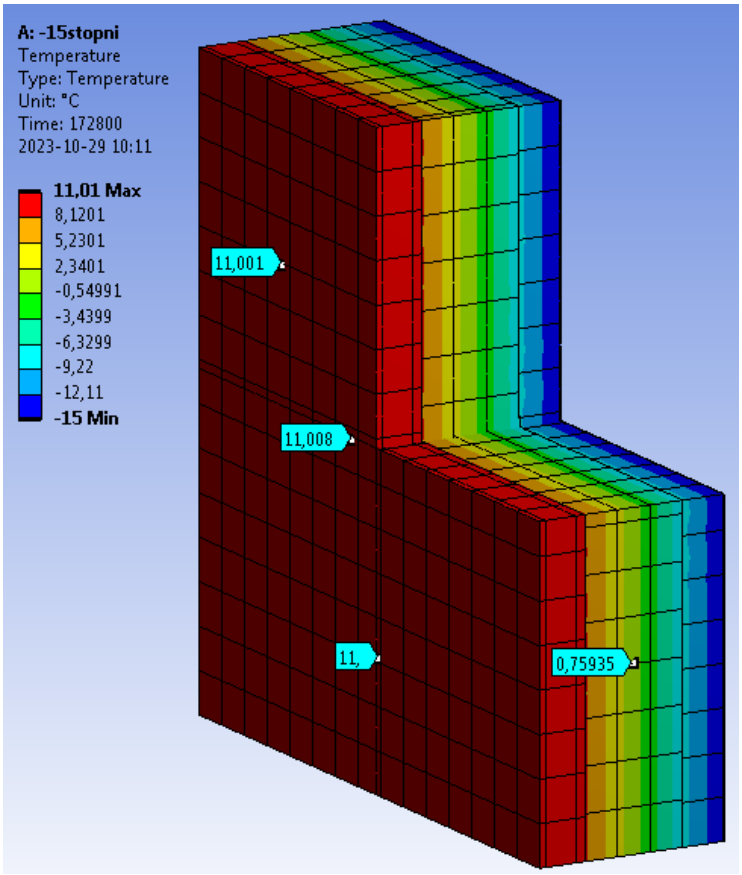

Fig. 6. Temperature distribution (°C) in the partition after 48 hours shown in cross-section

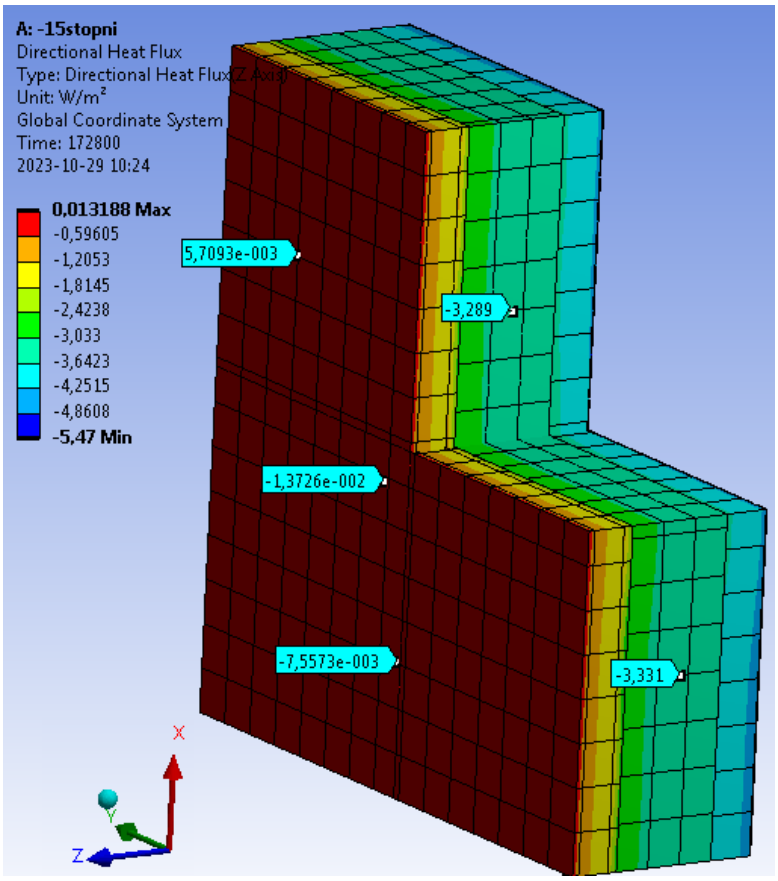

Fig. 7. Directional heat flux (Z axis) in the partition after 48 hours

Figure 7 shows the values of directional heat flux (in the Z axis, perpendicular to the planes of the layers). The obtained value of maximum heat flux of 0.013 W/m^2 on the Fermacell board (interior, residential side) indicates low heat loss compared to the previously studied partitions in the experimental and exploratory studies (for others configuration of the partition).

Figure 8 shows the values and direction of the total heat flux. It shows that the partition in the middle section has the highest heat loss (5.47 W/m^2). Compared to previously studied partitions, the value of the total heat flux decreased significantly from the value of 10.03 W/m^2 for the partition with a mineral wool filling through the value of 9.39 W/m^2 for the partition with a cellulose wool filling ending with the value of 8.98 W/m^2 for the partition with a wood wool filling (numerical analyses for the three partitions mentioned above were carried out for an external temperature of -12.5°C). The analysed partition, at the lower external temp. of -15°C shows an almost twofold decrease in the value for the total heat flux, thus translating into almost two times less heat loss inside the living area.

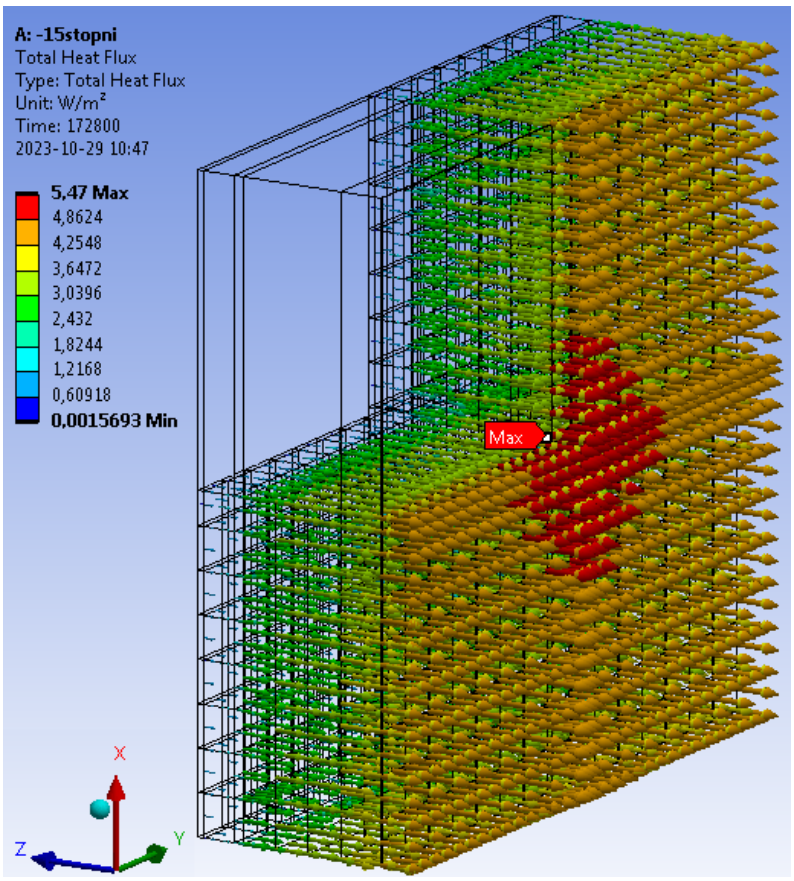

Fig. 8. Heat flux in the partition after 48 hours

Figure 9 shows the temperature distribution along the so-called path for the analysed temperatures (-15°C, -10°C, -5°C, 0°C, +5°C, +10°C, +15°C, +20°C, +25°C). The determined path ran exactly through the centre of the analysed partition (x = 0.6 m, y = 0.6 m). Vertical red lines, between which numbers 1 to 6 were inserted, marked the location of the inner partitions. The study assumed no heating in the interior of the building and only assumed a constant value for the temperature of the interior partition. The difference in temperatures on the inner partition results from the simulation time – 48 hours. For larger values, the difference would decrease.

It can be read from Figure 9 that for each range of outdoor temperature, proper stabilisation occurs in the last 3 partitions, namely OSB-3 board (designation 4 in Figure 9), Rockwool (designation 5 in Figure 9) and Fermacell board (designation 6 in Figure 9).

Figure 10 shows the distribution of heat flux (W/m^2) along the so-called path for the analyzed temperatures (-15°C, -10°C, -5°C, 0°C, +5°C, +10°C, +15°C, +20°C, +25°C). The determined path ran exactly through the centre of the analysed partition (x = 0.6 m, y = 0.6 m).

The vertical red lines, between which numbers from 1 to 6 were inserted, marked the location of the inner partitions.

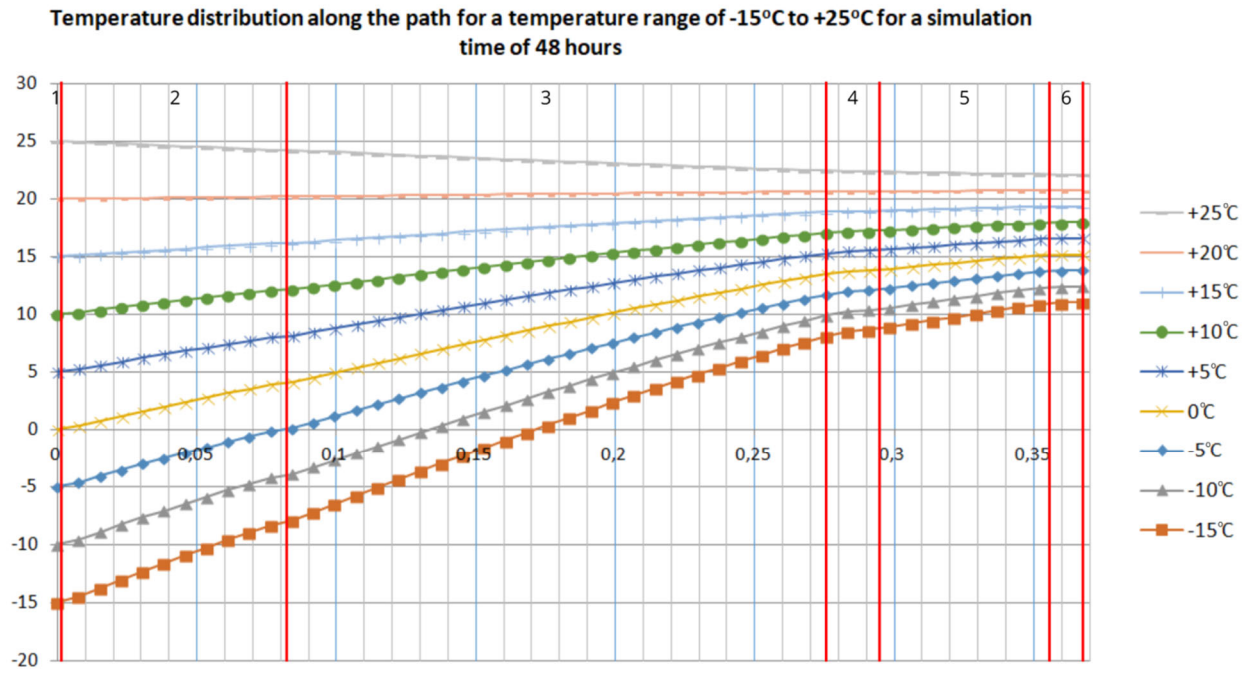

Fig. 9. Temperature distribution along the so-called path for the analysed temperatures (-15°C, -10°C, -5°C, 0°C, +5°C, +10°C, +15°C, +20°C, +25°C) with partitions marked: 1) Termoorganika white silicone plaster (adhesive+grid+plaster) 2 mm, 2) Steico Protect H-dry 80 mm, 3) construction filled with cellulose wool 195 mm, 4) OSB-3 18 mm, 5) Rockwool 60 mm, 6) Fermacell 12.5 mm

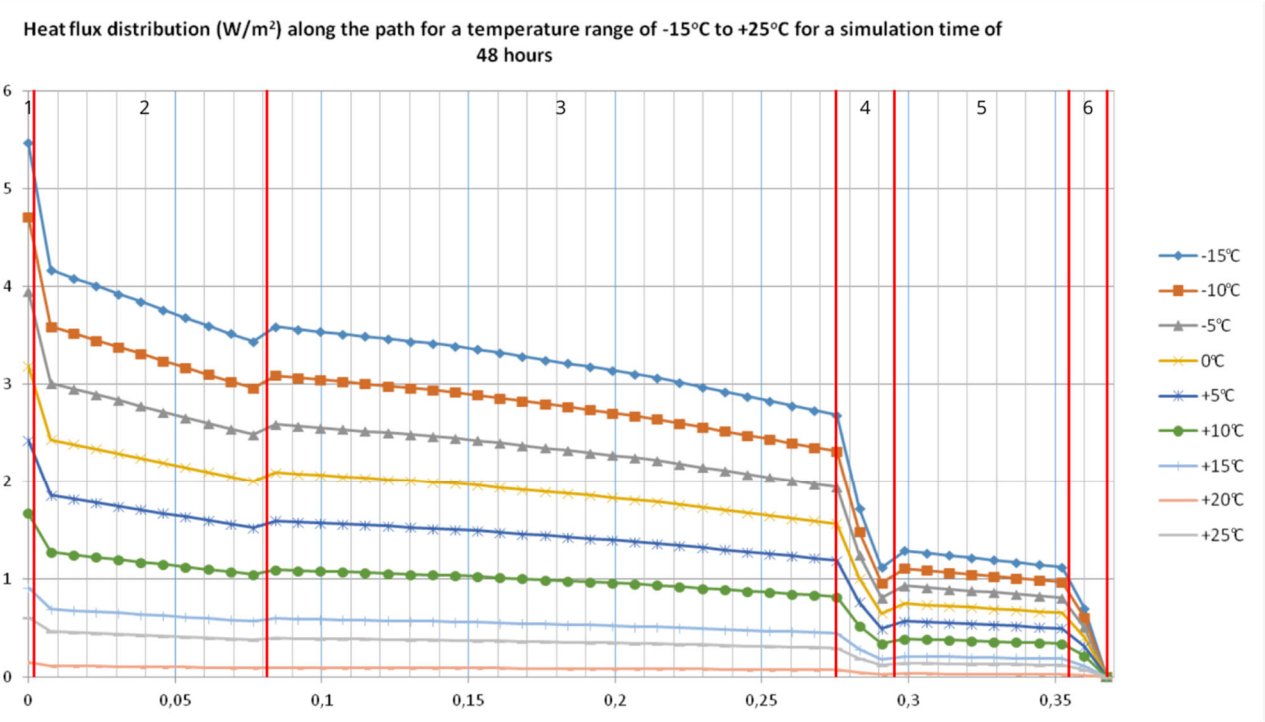

Fig. 10. Distribution of heat flux (W/m^2) along the so-called path for the analysed temperatures (-15°C, -10°C, -5°C, 0°C, +5°C, +10°C, +15°C, +20°C, +25°C) with partitions marked: 1) Termoorganika white silicone plaster (adhesive+grid+plaster) 2 mm, 2) Steico Protect H-dry 80 mm, 3) construction filled with cellulose wool 195 mm, 4) OSB-3 18 mm, 5) Rockwool 60 mm, 6) Fermacell 12.5 mm.

It can be read from Figure 10 that for each external temperature interval, proper stabilisation occurs in the last 3 partitions, that is, OSB-3 board (designation 4 in Figure 10), Rockwool (designation 5 in Figure 10) and Fermacell board (designation 6 in Figure 10).

During the comparison of the results of the numerical analyses with the selective readings taken during the year-round readings, it was noted that:

On July 30 at 9:00 am, the reading from sensor No. 2 (outdoor temp.) was 21.08°C. Sensor No. 7 (indoor temp) indicated a temp of 23.70°C. It was noted that there was a significant similarity with the results from the numerical analyses where, during the external temperature simulated at 20°C, the reading from the inside indicated a value of about 22°C after 48 hours. The difference settled at 6-7%.

On January 11 at 3 pm, the reading from sensor No. 2 (outdoor temp) was 4.96°C. Sensor No. 7 (indoor temp) indicated a temp of 21.69°C. A discrepancy was noted with the results from the numerical analyses where, during the external temperature simulated at 5°C, the reading from the inside indicated a value of about 17°C after 48 hours. The difference settles at 20%.

On February 13, at 11 pm, the reading from sensor No. 2 (outdoor temp.) was -0.05°C. Sensor No. 7 (indoor temp.) indicated a temp of 21.71°C. A discrepancy was noted with the results from the numerical analyses where, during an outside temperature simulated at 0°C, the reading from the inside indicated a value of about 17°C after 48 hours. The difference oscillates similarly to the previous case at 20%.

5. Conclusions

Comparison of the results from the computer simulations with the readings collected during the project at the experimental site allowed us to observe that some of the results are close to each other, but some differ at an average level of about 20%. The conclusions can be as follows:

The differences between the data from the real facility and the numerical analyses are due to the large amplitude of temperature changes during the winter, from minus temperatures at night to positive temperatures during the day. Numerical analyses indicated a given result after 48 hours, which in real conditions during the winter season is not quite possible to maintain.

The real object during the measurements, especially in the winter, could remain unheated inside for a certain period of its disuse to remain heated after a certain time through an air-conditioning system or other heat source. The simulations assumed a steady-state temperature at the inner partition of 21°C.

During the use of the facility, repeated opening and closing doors, i.e. continuous operation, could also have affected the values read from the sensors. In the numerical analyses, such a possibility was ignored.

During the summer, when temperatures were kept at the same level for a longer period, the results collected from the sensors were consistent with the results of the numerical analyses. This allows us to assume that the boundary and initial conditions for the simulation and the adopted material model are correctly selected.

Measurement differences on the order of 20% (up to as much as 50%) are natural in thermodynamics and generally acceptable. They do not affect the negative evaluation of computer simulations.

The results presented in the article are part of the experimental and numerical research carried out as part of an enterprise R&D project (proj. no. RPZP.01.01.00-32-0019/18). The R&D work conducted by ITS Sp. z o.o. and the Koszalin University of Technology Branch in Szczecinek concerned the creation of an optimal building envelope used in timber construction.

References

Charun, H. (2009). *Podstawy termodynamiki technicznej. Wykłady dla nieenergetyków, część 2*. Koszalin: Publishing House, Koszalin University of Technology. (in Polish)

Guzik, J. (2015). *Instalacje centralnego ogrzewania*. Krosno: Publishing House KaBe. (in Polish)

https://www.isover.pl/porady/zatrzymaj-cieplo-w-domu

Journal of Laws of the Republic of Poland (Warsaw, 9th June 2022) No. 1225. Obwieszczenie Ministra Rozwoju i Technologii w sprawie ogłoszenia jednolitego tekstu rozporządzenia Ministra Infrastruktury w sprawie warunków technicznych, jakim powinny odpowiadać budynki i ich usytuowanie. (in Polish)

PN-EN 13172:2012 (2012). Thermal insulation products – Evaluation of conformity.

PN-EN ISO 10456:2009 (2009). Construction materials and products standard. Thermal and humidity properties. Tabulated design values and procedures for determining declared and design heat values.

PN-EN ISO 6946:2008 (2008). Construction components and building elements. Thermal resistance and heat transfer coefficient. Calculation method.

Technical Conditions (2021)

Wiśniewski, S., Wiśniewski, T. (2017). *Wymiana ciepła*. Warsaw: WNT. (in Polish)